Article

pubs.acs.org/Biomac

Protein-Selective Coacervation with Hyaluronic Acid

Xiaosong Du,[†] Paul L. Dubin,*[,‡] David A. Hoagland,[†] and Lianhong Sun[§]

[†]Department of Polymer Science and Engineering and [‡]Department of Chemistry University of Massachusetts, Amherst, Massachusetts, 01003, United States

[§]School of Life Sciences, University of Science and Technology of China, Hefei, Anhui, People's Republic of China, 230027

Supporting Information

ABSTRACT: Selective coacervation with hyaluronic acid (HA), a biocompatible and injectable anionic polysaccharide, was used to isolate a target protein, bovine serum albumin (BSA), with 90% purity from a 1:1 mixture with a second protein of similar pI, β-lactoglobulin (BLG). This separation was attributed to the higher HA-affinity of BSA, arising from its more concentrated positive domain. The values of pH corresponding respectively to the onset of complex formation, coacervation, precipitation, and redissolution (pH_c, pH_ϕ, pH_p, and pH_d) were determined as a function of ionic strength I. These pH values were related to critical values of protein charge, Z, and their dependence on I provided some insights into the mechanisms of these transitions. The higher polyanion binding affinity of BSA, deduced from its higher values of pH_c, was confirmed by isothermal titration calorimetry (ITC). Confocal laser microscopy clearly showed time-dependent coalescence of vesicular droplets into a continuous film. Comparisons with prior results for the polycation poly(diallyldimethylammonium chloride) (PDADMAC) show reversal of protein selectivity due to reversal of the polyelectrolyte charge. Stronger binding of both proteins to PDADMAC established by ITC may be related to the higher chain flexibility and effective linear charge density of this polycation.

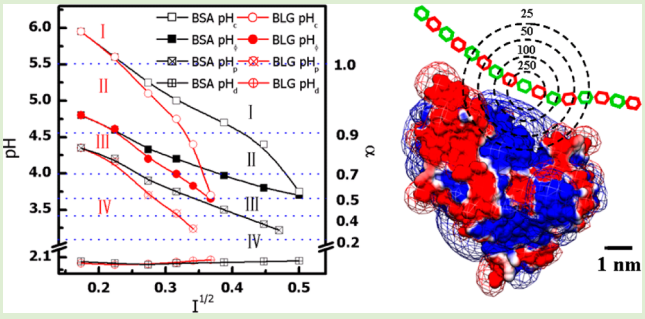

INTRODUCTION

Extensive studies have established selective interactions of synthetic polyelectrolytes (PE) with proteins[1] that can lead to biotechnological applications such as efficient purification of proteins.[2] As biodegradable and environmentally friendly materials, natural PEs like charged polysaccharides,[3] may offer better methods of coacervation-based protein purification. In particular, hyaluronic acid, an anionic polysaccharide and approved injectable, offers particular advantages for the purification of protein drugs. However, relatively little is known about the relationship between protein-specific affinity and selective coacervation for weak PEs with pH-dependent charge.[4,5]

In spite of the growing demand for recombinant proteins,[6] protein purification is usually an expensive and slow process.[7] Currently, commercial separation techniques include liquid chromatography and membrane separation. Liquid chromatography is limited by its low-yield and large solvent consumption.[8] Membrane-selective separation is limited by the low binding capacity of proteins and the quality of the membranes.[9] Therefore, large-scale and economic separation techniques are needed. Efficient and highly selective protein separation via coacervation provides an important alternative to traditional methods. Another attractive feature of this "soft method" is that protein stability and bioactivity can be retained during the separation process.[10]

PE/protein complex coacervation is a liquid–liquid phase separation occurring through nonspecific electrostatic interactions. For protein–PE systems, the protein charge density is pH-dependent, and a critical pH marks the onset of binding of proteins to polymer chains.[11] While this "pH_c", corresponding to an ionic-strength dependent critical local protein surface charge density, may occur when the two macromolecules have the same charge sign,[12] phase separation (coacervation) at "pH_ϕ" requires that the charge of the bound proteins compensates for the charge of the PE.[13] While this neutralization overcomes repulsion among like-charge complexes, the actual driving force for coacervation is the entropy increase from counterion release.[3−14] Centrifugation or settling then separates the dilute equilibrium supernatant from a more concentrated dense phase "coacervate" that can contain a target protein whose pH_ϕ deviates significantly from other proteins present in the same system.

Within multiprotein systems, a target protein with higher PE affinity might be proposed to coacervate more efficiently, that is, pH_ϕ depends on pH_c; however, while protein net charge influences the former, protein charge anisotropy determines the latter. In fact, proteins of nearly equal pI can show wide differences in pH_c. The observation of pH_c "on the wrong side of the isoelectric point" suggests the role of a "charge patch", a

Received: October 10, 2013
Published: February 1, 2014

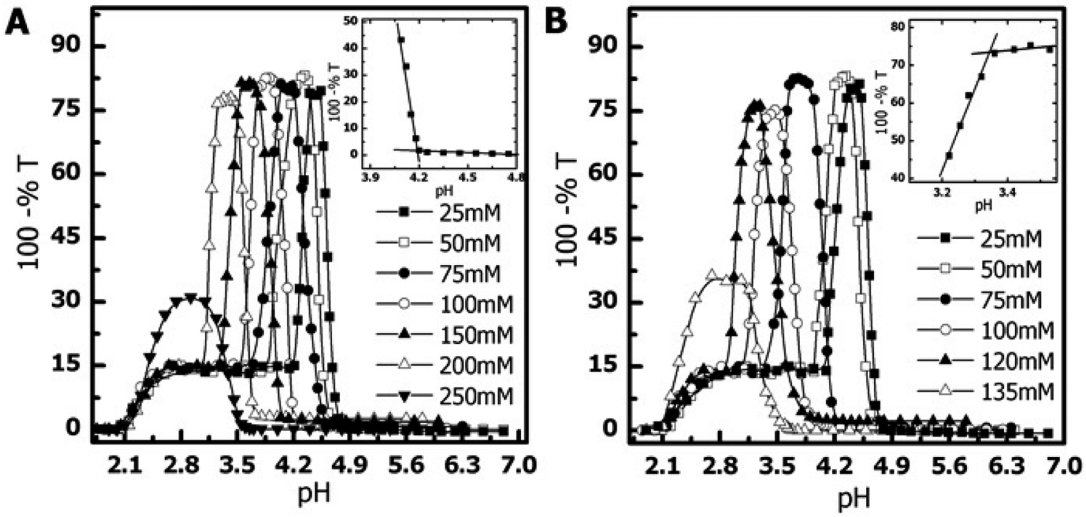

Figure 1. Turbidimetric titration of (A) HA/BSA and (B) HA/BLG solutions at different ionic strengths: protein and polymer concentration are 0.5 and 0.05 g/L, respectively. pH_ϕ and pH_p are determined as points of departure from lines of zero slope, shown in the insets of (A) for pH_ϕ of BSA; and (B) for pH_p of BLG, both at 100 mM salt.

protein region with a local charge density opposite to the global charge.[11−15] Bovine serum albumin (BSA) with a positive domain binds the strong polyanion poly(acrylamidomethylpropyl sulfonate) at pH 6.9 (2.0 pH units above pI),[11] but the onset of polyanion binding for β-lactoglobulin (BLG) at pH 6.2 occurs at pH − pI = 1.0.[16] Through electrostatic modeling, an identical region of positive potential (∼5 Å from the BSA surface) was found to appear at various conditions of pH and salt concentration.[15] The charge anisotropy of a protein defines its "charge complementarity" with a polyelectrolye partner, as influenced by the charge sequences and chain stiffness of the latter. This interaction, a combination of short- and long-range forces, is to be distinguished from site-specific recognition as for DNA−protein interactions. The consequence of charge complentarity in terms of separation is shown by the ability of the flexible polycation poly(diallyldimethylammonium chloride) (PDADMAC) to preferentially coacervate BLG from BSA despite the higher pI of the former (5.2 vs 4.9).[2]

In this paper we test the hypothesis mentioned above − the relationship among protein charge anisotropy, pH_c, pH_ϕ, and selective coacervation − using hyaluronic acid (HA) to complex with and separate the two proteins BSA and BLG. While the corresponding values of pI (4.9 and 5.2) are similar, BSA has a well-defined positive domain (lacking in BLG); and BSA is susceptible to unfolding at low pH. We use turbidimetric titration to establish conditions for the formation of various phases whose boundaries are defined by pH_c and pH_ϕ, as well as conditions for precipitation, interestingly reversible in this case. Calorimetry is employed to compare the thermodynamic parameters for the complexation of the two proteins. The impact of PE chain stiffness and charge density/sign is assessed by comparison with previous results for these two proteins with the more flexible and higher charge density synthetic polycation PDADMAC.[2] As a weak polyacid, the charge density of the HA chain is sensitive to pH, whereas PDADMAC has a constant charge density through all pHs. Examination of the HA/protein system can lead to a better understanding of protein binding to weak PEs with a pH-dependent charge.

EXPERIMENTAL SECTION

Materials. Hyaluronic acid (HA, MW 9 × 10^5), produced by streptococcus bacteria and purified by filtration through activated charcoal, was a gift of Shiseido Co. (Japan). BSA (68 kDa) with total free acid content ≤1.2 mg/g was from Roche Diagnostics (Indianapolis, IN; CAS 9048−46−8). BLG (18 kDa, referred to below as "native BLG") was a gift from C. Schmitt (Nestle, Lausanne). NaCl, sodium acetate, sodium phosphate (monobasic), and standard NaOH, HCl, and acetic acid solutions were purchased from Fisher Scientific. Milli-Q water was used in all sample preparation. Fluorescein isothiocyanate (FITC) and rhodamine B isothiocyanate (RITC) were from Sigma-Aldrich (Milwaukee, WI).

Turbidimetric Titrations. Highly precise turbidimetric titrations (%T ± 0.05%) were carried out for solutions containing proteins and polyelectrolytes in order to determine the points of complex formation and phase separation (pH_c, pH_ϕ). At the temperature range of 23−25 °C, no temperature effect could be seen. HA solutions (0.1 g/L, 1.1 × 10^{-7} mol/L), BSA protein (1 g/L, 1.5 × 10^{-5} mol/L), and BLG protein (1 g/L, 5.5 × 10^{-5} mol/L) were prepared separately at the desired concentrations of NaCl (25−250 mM), filtered (0.22 μm Millipore), and then mixed at equal volumes to give 10 mL. Addition of 0.01 N HCl with a 2.0 mL Gilmont microburet to a final pH of 2 in increments of ∼0.1 pH units, with simultaneous monitoring of pH and transmittance (T), was done while stirring at a speed of about 1000 rpm. Transmittance was measured using a Brinkmann PC 800 colorimeter equipped with a fiber optics probe (optical path length b = 2 cm) and a 450 nm filter, and pH was measured with a Corning 240 pH meter. For convenience, the turbidity $\tau = -\ln T/b$, is replaced by 100%T, which can easily be shown to be linear with τ at %T > 85. The titration was completed within 15 min to minimize effects of BLG aggregation. After suitable warm-up, the instrument drift over this time period was verified as less than 0.15 transmittance unit/h. It is important to note that solutions with 100%T < 10 (e.g., Figure 1) are typically optically clear.

Preparation of Mixed Coacervates. To observe separation of BSA and BLG as a consequence of HA binding and coacervation, BSA, BLG and HA were all mixed together in pH 7, I = 200 mM (NaCl) to yield a solution 5 g/L in BSA, 5 g/L in BLG, and 0.5 g/L in HA. The mixed coacervatate was formed by pH adjustment to 3.5. The resulting turbid suspension was centrifuged (Beckman Coulter Allegra 6R, swing-bucket rotor) for 1 h at 4000 rpm (corresponding to a relative centrifugal field of 3650 × g), 20 °C to produce optically clear dilute (upper) and dense (lower) phases (supernatant and coacervate, respectively).

dx.doi.org/10.1021/bm500041a | Biomacromolecules 2014, 15, 726−734

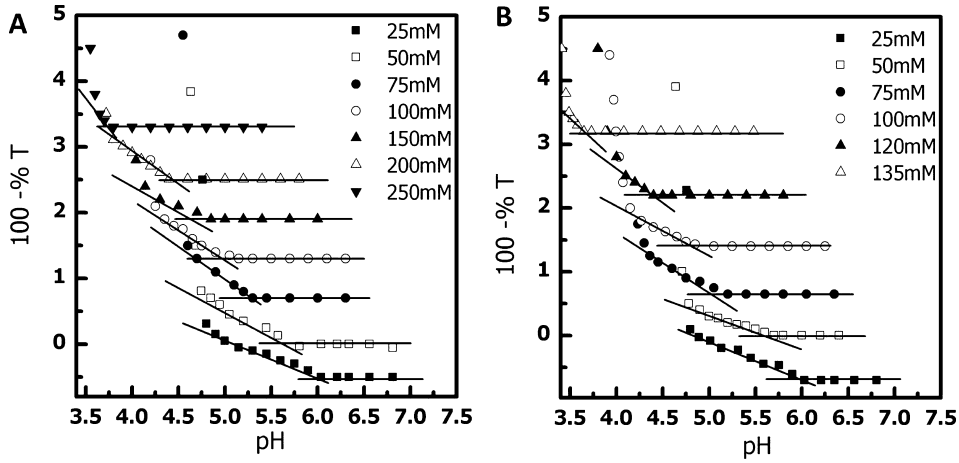

Figure 2. Determination of transitions from noninteracting solution to soluble complex (pH_c) for HA with (A) BSA and (B) BLG at different ionic strength corresponding to soluble complex formation (pH_c). Protein and polymer concentrations are 0.5 and 0.05 g/L, respectively.

Size Exclusion Chromatography. To investigate protein compositions in coacervate and supernatant, we carried out SEC on a prepacked Superose 6 HR 10/30 column using a Shimadzu Prominence LC system equipped with a refractive index detector (RID-10A) with 20 μL injections. The mobile phase was 150 mM NaCl + 30 mM Tris buffer (pH 7) at 1 mL/min. Solutions were filtered (cellulose acetate) prior to injection (20 μL). The coacervate was analyzed by dissolving 0.1 g of the dense phase in 0.4 mL of 0.2 M NaCl adjusted to pH ~ 7.

Confocal Laser Scanning Microscopy. FITC-labeled BSA and RITC-labeled BLG were prepared by reaction of FITC/RITC isothiocyanate group (−N═C═S) with protein amine.[17−20] The fluorescein dye was attached to protein by the thiourea bond. We prepared a solution of 2 g/L of protein in DI water and dissolve the FITC/RITC in anhydrous DMSO at 1 g/L. Protein or polymer was then mixed with FITC/RITC dye in a volume ratio of 20:1. The coupling reaction was carried out in the dark for 8 h. Free fluorescence dye was removed by dialysis followed by freeze-drying. The ratio of fluorescein dye to protein was ~0.5, obtained by measuring the absorbance at 495 and 280 nm. The fluorescence images were taken with a Leica TCS SP confocal laser scanning microscope with a 50× objective lens in the transmission mode. Emission spectra of FITC- and RITC-labeled proteins were taken over 500−530 and 590−620 nm, respectively, with excitation at, respectively, 488 and 548 mm.

Computational Methods. Computer modeling was used to visualize the electrostatic potential around the protein as a function of pH and ionic strength. DelPhi V98.0 (Molecular Simulations) was used to calculate electrostatic potential around the protein by nonlinear solution of the Poisson−Boltzmann equation.[21] The protein crystal structures with Protein Data Bank identifications 1AO6 (BSA) were taken from the RCSB Protein Data Bank (http://www.rcsb.org). The charges of amino acids were generated using the spherical-smeared-charged model proposed by Tanford[22] utilizing the protein titration curve of proteins.[23,24]

Isothermal Titration Calorimetry. ITC was carried out using a model VP-ITC (Microcal, Northampton, MA). Both protein and polymer solutions to be used in HA experiments were made in pH 4.3 buffer containing 10 mM phosphate and 90 mM NaCl. All solutions were filtered (0.22 μm Millipore). After instrument stabilization for at least 1 h at 25 °C, 40 successive 6 μL injections of 1.4 mM BSA or BLG at intervals of 400 s were used to titrate 1.445 mL of 1.1 and 1.5 g/L HA, respectively, with stirring at 315 rpm. Prior to data analysis, heats of dilutions were corrected by subtracting values for polymer-free blank solutions. ITC data analysis requires (1) conversion of raw calorimetric data (heat evolved or consumed for each titration step, $\delta\Delta H^\circ$) to a binding isotherm, and (2) model-dependent fitting of the binding isotherm to yield binding site number (size) and binding constants from which ΔG° and, hence, ΔS° can be obtained. The first step (1) is based on the assumption that any decrease in $\delta\Delta H^\circ$ relative to its initial value is due to incomplete binding of the titrant molecules. In Microcal software, step (2) follows a particular model of protein−ligand interactions based on single site binding or multiple identical sites. In our case, the protein is the ligand and many protein-binding sites on the polyelectrolyte can affect each other in various cooperative and anticooperative ways. Following previous literature,[25,26] thermograms were transformed into binding isotherms. Then the binding isotherms were fit by the McGhee−Von Hippel model,[27] which describes the binding of interacting or independent ligands (proteins) to a homogeneous one-dimensional lattice (polyelectrolyte). The binding model takes on the following form:

$$\frac{\nu}{L} = K_{obs}(1 - n\nu)\left[\frac{1 - n\nu}{1 - (n-1)\nu}\right]^{n-1} \quad (1)$$

where ν represents the binding density, that is, the number of proteins bound per polymer unit, L is the free-protein concentration, n is the binding site size (number of polymer units per bound protein molecule), and K_{obs} is the intrinsic binding constant.

RESULTS AND DISCUSSIONS

As shown in Figures 1 (insets) and 2, these turbidimetric titrations can be used to determine the pHs of soluble complex formation (pH_c) and liquid−liquid phase separation (pH_ϕ). Differences in binding affinity of BSA versus BLG, qualitatively observed from the pHs of complex formation in Figure 2, lead to differences in the pHs of coacervation from Figure 1. While BSA is believed to undergo unfolding below pH 4,[28,29] this does not appear to directly affect complex formation in that the region of noninteraction (zero slope in Figure 2A) which defines pH_c is clearly defined for I = 250 mM, where pH_c is observed at pH = 3.7. Direct comparison of Figure 2A and B shows that the onsets of binding for BSA and BLG are identical at I < 75 mM, but at higher ionic strength, values of pH_c are higher for BSA meaning that it binds to HA more strongly. $pH_c^{BSA} - pH_c^{BLG}$, which expresses the higher HA affinity of BSA at I > 75 mM, ranges from 0.3−1.0 for 75 < I < 135 mM. This leads to $pH_\phi^{BSA} > pH_\phi^{BLG}$, which indicates selective coacervation of BSA as the pH is adjusted downward in the presence of HA. The difference in affinity is sufficiently large at high ionic strength so that the more weakly binding protein does not affect the binding of the stronger one, as seen from the identical titration curves for HA/BSA in the presence and absence of BLG at $I \geq$ 100 mM (Figures S1 and S2). Even though the difference in affinity is greatest at high salt, the low values of the turbidity maxima for the two proteins at the

dx.doi.org/10.1021/bm500041a | Biomacromolecules 2014, 15, 726−734

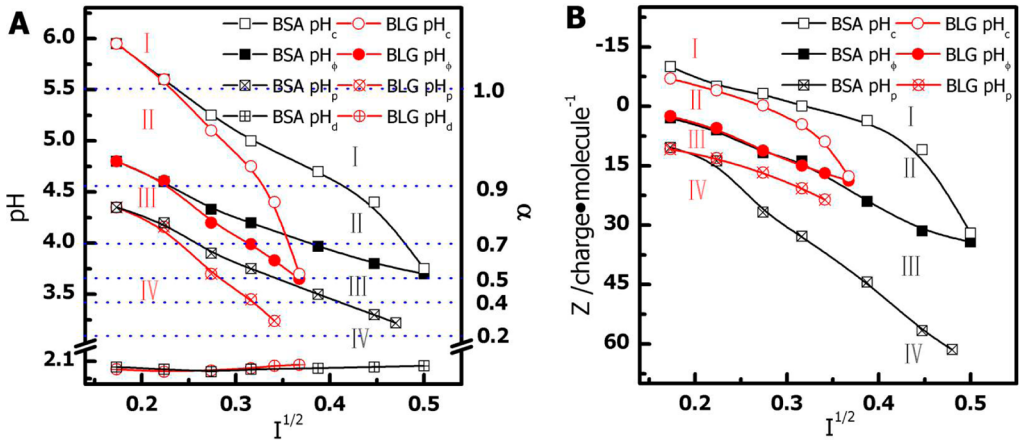

Figure 3. (A) Phase boundaries of BSA and BLG with HA from data of Figures 1 and 2. The *y*-axis on the right shows the degree of ionization HA, α. (B) Ionic strength dependence of protein net charge based on potentiometric titrations of BSA[23] and BLG.[24] pH$_c$, pH$_\phi$, pH$_p$, and pH$_d$ stand for pH values of soluble complex, phase transition, precipitation, and redissolution, respectively. Domains I–IV stand for noninteracting, soluble complex, coacervate, and precipitate, respectively.

highest salt concentrations suggest incomplete coacervation of protein/polyanion complexes, to the extent that solutions with both proteins remain optically clear at all pHs at salt concentrations above those in Figure 2. The important point is that the greater HA affinity of BSA versus BLG allows the first to be selectively coacervated from the second in the range of 75 to 135 mM salt.

As the pH is decreased further below pH$_\phi$ at fixed I < 150, cotton-like structures appear, and a third transition can be observed, operationally defined as in the inset of Figure 1B by the onset of a steep negative slope (dτ/dpH). This "pH$_p$" resembles the transition from fluid to solid in coacervate droplets observed microscopically for BSA/PDADMAC at high pH[30] and designated as pH$_{precip}$. The cooperativity of this process is not as well understood as the reversible phenomena pH$_c$ or pH$_\phi$. Even more complex kinetics must be involved in the process of redissolution of the precipitate, which we observe after several minutes of stirring at ∼pH 2 at which condition the unfolding of BSA might play a significant role. The fact that precipitation is suppressed at low pH should be attributed to zero number of COO$^-$ per HA repeat unit for pH ≪ pK_a (∼2.8) where electrostatics are less important. The ease with which the precipitate redissolves at pH 2 seems to suggest that extensive denaturation of the protein does not occur, even though CD shows that HA stabilizes a comformer with less secondary structure at pH <3.5. This process was observed to be reversible with respect to pH, consistent with protein resistance to acid denaturation.[31]

Conditions for selective coacervation are established by the phase boundaries in Figure 3A, which show the ionic strength dependences of critical pH values pH$_c$ and pH$_\phi$, determined as described above. The dependence of protein net charge Z on I at critical conditions is also shown in Figure 3B in order to examine the phase boundaries from an electrostatic point of view. The effect of salt on the different critical values is shown in terms of $I^{1/2}$, in view of the assumed role of the screening length, κ^{-1} (nm) ∼ 0.3/$I^{1/2}$. Figure 3A is constituted of multiple titrations each at fixed ionic strength, reflecting, for example, at I = 100 mM, the fact the addition of HCl to BSA/HA results in (1) complex formation at pH ∼ 5.0 (transition from noninteracting region I to complexation in region II), (2) coacervation at pH ∼ 4.2 (transition from region II to the liquid–liquid biphasic region III), and (3) the formation of a precipitate (region IV) at pH 3.8, which finally will redissolve at pH ∼ 2. These figures may not constitute phase boundaries in the traditional equilibrium sense, but in Figure 3A they provide guidance for choosing conditions for optimal separation by coacervation, namely, conditions in which only one protein has entered region III. The region centered around pH 4.0 and 100 mM ($I^{1/2}$ = 0.33) satisfies this requirement but is too narrow to be effective, so that optimal conditions for selective coacervation of BSA are close to pH 3.5/200 mM (with higher ionic strengths producing smaller coacervate yield). While the low-pH expansion of BSA deduced in ref 25 from the very limited data then available has been reinforced somewhat erratically by more recent studies, it is noteworthy that no feature of Figure 2A or 3A reveals any discontinuities for BSA in the pH 3–4 range nor any behavior dissimilar to that seen for BLG. Similarly, the convergence of the redissolution regions of BSA and BLG argue against attributing that behavior to acid-induced expansion of the former.

The boundaries of Figure 3A,B also inform us about the origin of coacervation selectivity, in particular, its relationship to protein-HA affinity, that is, the relationship between pH$_c$ and pH$_\phi$. Selective coacervation is seen to be lost at I < 50 mM (pH$_\phi$ values for the two proteins become identical), where the difference in pH$_c$ also vanishes. The II/III boundary for BLG (red filled circles in Figure 3A) diverges from the II/III boundary for BSA (black filled squares) at I > 50 mM. In this regard, it follows the divergence of the I/II boundaries (open red circles, blacks squares). Figure 3B shows similar trends although less obviously. Coacervation selectivity, qualitatively measured by the vertical difference between the coacervaion boundaries (II/III) of BSA and BLG in Figure 3A increases with I in the range 3.7 < pH < 4.3. When pH changes from 4.3 to 3.7, the net charges of BSA and BLG increase from +10 to +33 and from +10 to +17, respectively. In Figure 3A, the maximum divergence of coacervation pH$_\phi$ is seen at I = 135 mM ($I^{1/2}$ = 0.37), and this is aligned with the maximum divergence of pH$_c$; but while the difference in pH$_c$ is almost one pH unit, the difference in pH$_\phi$ is only about 0.3 pH units. This distinction is even more noticeable in Figure 3B at the same ionic strength, where the II/III (Z_ϕ) boundaries for the two proteins actually converge, even when the I/II (Z_c) boundaries

dx.doi.org/10.1021/bm500041a | *Biomacromolecules* 2014, 15, 726–734

are well separated. This means that net protein charge is more important than charge patch for the II/III boundary, that is, charge anisotropy does not play a dominant role for the II/III boundary. The value of pH_c for BSA is typically higher than BLG (Figure 3A); and BSA binds HA more strongly than does BLG of the same net charge at any give ionic strength (Figure 3B). Nevertheless, at the relevant ionic strengths, the tendency of BSA to coacervate is identical to the coacervation tendency of BLG with the same net charge (congruence of the II/III boundaries if Figure 3B). Thus, complexation and coacervation orginate from different driving forces, the former from the local interaction between HA and the protein domain and the latter from more long-range interactions between complexes. Put differently, pH_c or Z_c qualitatively describe the PE-protein binding affinity, that is, the binding constant that determines the degree of occupancy of the protein-binding sites on the polymer.[2] If the condition for coacervation is complex charge neutralization,[13] it can be described by

$$Z_T = 0 = Z_{PE} + nZ_{Pr} \quad (2)$$

where Z_T is the total charge of polymer chain bound by proteins, Z_{PE} is the charge of polyelectrolyte, Z_{Pr} is the charge of protein, and n is the number of proteins bound per polymer chain and depends on its binding constant and free protein concentration. Z_{PE} is a linear function of α (the degree of ionization of HA) and Z_{Pr} is a protein-specific function of pH. However, n_ϕ depends both on the binding constant and the protein charge and these two effects are difficult to resolve at pH < pI. The higher binding affinity due to charge anisotropy may increase n for BSA, but its higher value of Z_{Pr} leads to a lower value for n_ϕ, and two effects (affinity and net charge) may compensate.

Affinity may be considered from a more local point of view. To consider the effect of ionic strength on the local interaction between HA and the BSA protein domain, Figure 4 schematically represents the regions of the HA-BSA complex unscreened by added salt, where the radii of the dashed circles correspond to the screening length $\kappa^{-1} \sim 0.3/I^{1/2}$. At I = 85 mM, the I/II boundaries of BSA and BLG begin to diverge: at equal Z, more salt is needed to dissociate BSA than BLG. However, at lower I, corresponding to $\kappa^{-1} > 1$ nm from the protein surface, they converge; the charge patch plays a lesser role in binding. The schematic of Figure 4 suggests that when I < 50 mM, more than three repeat units (disaccharides) of HA are within the potential domain of the protein. This means that interactions beyond the protein positive patch become important; selectivity is therefore lost because HA begins to interact repulsively with charges outside of the "patch", that is, distinctive features of the positive domain (charge patch) of BSA become less significant.

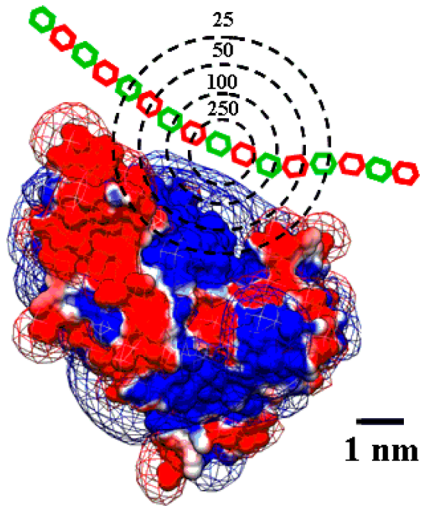

Figure 4. Schematic diagram represents the regions of the HA-BSA complex unscreened by added salt, where the radii of the dashed circles correspond to the screening length κ^{-1} over the ionic strength range 25−250 mM. The length of each disaccharide unit is 1.3 nm. Electrostatic potential contours of BSA protein represented as blue (+0.5 kT/e) and red (−0.5 kT/e) at pH 4.3, I = 100 mM. Negatively charged and neutral glucose units of HA were represented as red and green hexagons, respectively. No comparable diagram can be presented for BLG which lacks a unique positive HA-binding domain.

The pH_c and pH_ϕ curves define the regions of soluble complex formation for the two proteins, but these regions disappear at high salt, notably at the same pH ∼ 3.7. Because Figure 3B shows that the values of Z_c for BLG and BSA are not the same at this condition, we turn to the HA charge as the point of similarity: complexation for either protein is no longer possible when the degree of ionization of HA[32] is less than α = 0.5. Put differently, an increase in protein positive charge does not compensate for the loss of HA charge when the distance between HA charges is greater than 2 nm. Similar effects have been seen for other weak polyanions in previous work[4,5] but only partially analyzed. The interrelationship between HA charge and protein charge at critical binding conditions has a fundamental basis in theories put forward for systems less complex than proteins and can be applied to proteins if the effective local surface charge density of the protein can be known.[33] Consideration of the effect of PE linear charge density conjoined with a variation in protein charge can be expressed semiempirically through a general relation for the critical condition for polyelectrolyte adsorption on surfaces of opposite charge:

$$\sigma^a \xi^b \sim \kappa^c \quad (3)$$

where σ is the colloidal (here protein) effective surface charge density, ξ is the charge per polymer repeating unit here the HA disaccharide, and κ is the Debye−Hückel parameter.[34,35] The requirement for more positive protein charge at low α follows directly from eq 3. The evaluation of the scaling terms could in principle be undertaken here on the basis of the set of values of α, Z, and I corresponding to pH_c. This approach, beyond the scope of the present work, will be the subject of future studies. Another interesting feature are the slopes for BSA and BLG in Figure 3, which are measures of the amount of salt needed to desorb HA when the protein charge has increased in the positive direction from the pH_c boundary by some given amount in Z. Both Figure 3A and B indicate that complexes and coacervates with BSA are more resistant to dissolution by salt. The decrease in slope at I = 100 mM for BLG and at 200 mM for BSA correspond to conditions at which the change in pH needed to compensate for the addition of salt becomes greater; that is, an increase in Z per unit positive charge becomes less effective for salt resistance. This is expected to occur when positive charges are no longer added exclusively to the charge patch.[36] The validity of eq 3 has been tested for BSA and strong polyanions[36] in which a linear dependence of protein net charge on $I^{0.45}$ (along with binding "on the wrong side of pI") was rationalized with the speculation that all positive charges at low pH did involve the same "positive patch". This analysis

dx.doi.org/10.1021/bm500041a | Biomacromolecules 2014, 15, 726−734

could not be relevant to conditions of BSA unfolding at pH < 3.5, but this only affects the data points above I = 400 mM in Figure 3A,B.

The onset of precipitation (region IV) is expected to occur more readily (at a higher pH), for low ionic strength, and for the higher HA-affinity protein, BSA. In fact, in Figure 3A the II/III boundaries appear to parallel the III/IV boundaries, both for BSA and BLG; that is, the precipitation domain is more extensive for BSA. This similarity of ionic strength dependences implies that the forces responsible for the formation of precipitate are similar to the forces involved in coacervation, that is, involving both local and global charges. In this sense, precipitation might be viewed as a continuation of coacervation, that is, further loss of solvation due to strong interactions at low salt. However, differences between BSA and BLG pH/I phase boundaries could arise somewhat trivially from the large difference in their protein net charge. For this reason, we turn to Figure 3B, in which comparisons are made at fixed Z, a more fundamental parameter than pH. While the I/II boundaries in Figure 3B indicate stronger complex formation for BSA, and the II/III boundaries suggest equivalent tendencies to coacervate (at fixed Z), that is, the III/IV boundaries are inverted: they appear to suggest that further progression to precipitate is favored for BLG but more directly point out that BLG at the onset of precipitation has a smaller global positive charge. Despite its lower positive charge, the surface charge density ratio is somewhat larger for BLG (especially if there is partial unfolding of BSA), and the volume charge density is almost twice as large. This leads to greater ion-pairing and counterion expulsion, thus, desolvation; that is, precipitation occurs more readily. The markedly different III/IV boundaries for BLG and BSA in Figure 3B are clarified through their inverse slopes $(dZ/dI^{1/2})^{-1}$, that is, $\Delta I^{1/2}_{p}$, the amount of salt required to reverse precipitation arising from an increase in protein net charge. In this way, identical increases in Z have a stronger precipitating effect for BLG. It is of interest to note the remarkably uniform dependence of Z_p on $I^{1/2}$ for BSA; this suggests that the addition of some particular number of charges has the same effect on $\Delta I^{1/2}_{p}$, regardless of the positions of those charges. This implies a dominant role for net protein surface charge density.

This viewpoint explains how BLG's higher global surface charge density can lead to a more robust precipitate. However, the absence of even complex formation for BLG at I > 135 mM precludes the formation of any dense phase for this protein at high salt. For BSA, the III/IV boundary in Figure 3B is seen to terminate at Z = +60, I = 250 mM. This data point represents the limiting condition for precipitation, which extends beyond the limiting condition for coacervation or complex formation: Both of these are impossible at α < 0.5, but precipitation can occur at α below 0.3. Despite the low HA charge density, HA flexibility may be sufficient for the polymer to conform to the globally positive protein in a such a way that the number of HA-protein "ion pairs" increases more dramatically for the coacervate–precipitate transition than for complexation. Put differently, while the number of COO^- per HA repeat unit is small at low pH, all of them can be within the regions of positive protein potential which is large at low pH. On the other hand, precipitation is totally suppressed at pH 2; here all precipitates redissolve in the vicinity of α = 0, where electrostatics are less important. While PE-protein precipitation is common and selective precipitation has been suggested as a means of protein separation,[37] facile recovery from coacervate requires less extreme conditions.

Microscopic observation reveals both separation efficacy and large-scale changes in liquid–liquid suspension formed from a mixture of HA with BSA and BLG, labeled with FITC and RITC, respectively. As shown in Figure 5, the protein-rich

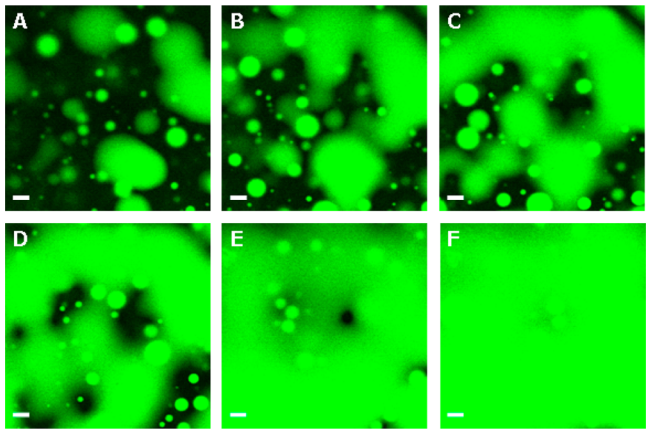

Figure 5. Fluorescence images of the ternary coacervate by confocal laser microscope as a function of time (seconds): (A) 80, (B) 140, (C) 260, (D) 400, (E) 550, and (F) 700 after mixing RITC-BLG/FITC-BSA/HA at pH 3.5; I = 200 mM. Scale bar 10 μm.

coacervate mainly comprises the FITC-labeled BSA. After ~10 min, a continuous coacervate film appears to form, in part as a consequence of the fusion of large droplets and subsequent sedimentation, for example, Figure 5C. A more quantitative analysis of protein separation by coacervation at pH 3.5, I = 200 mM, was obtained by SEC of supernatant and redissolved coacervate. Figure 6 shows SEC chromatograms for the supernatant, the control, and the redissolved coacervate phase. The peaks at 24 and 27 min correspond to BSA and BLG, respectively. The efficiency or yield of BSA coacervation with PE (the percent of the target protein in the coacervate) is

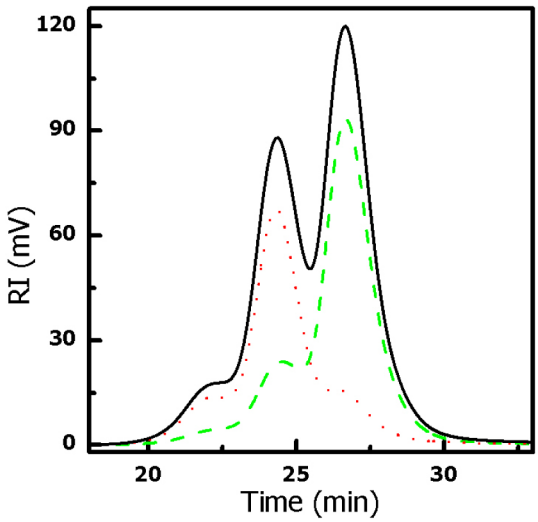

Figure 6. SEC analysis of proteins in different phases separated at pH 3.5, I = 200 mM. (a) 1:1 BSA/BLG total protein 10 g/L (prior to interaction): black solid line; (b) supernatant, filtered and injected: green dashed line; and (c) coacervate: red dotted line. The elution of HA at about 5 min is not shown.

dx.doi.org/10.1021/bm500041a | Biomacromolecules 2014, 15, 726–734

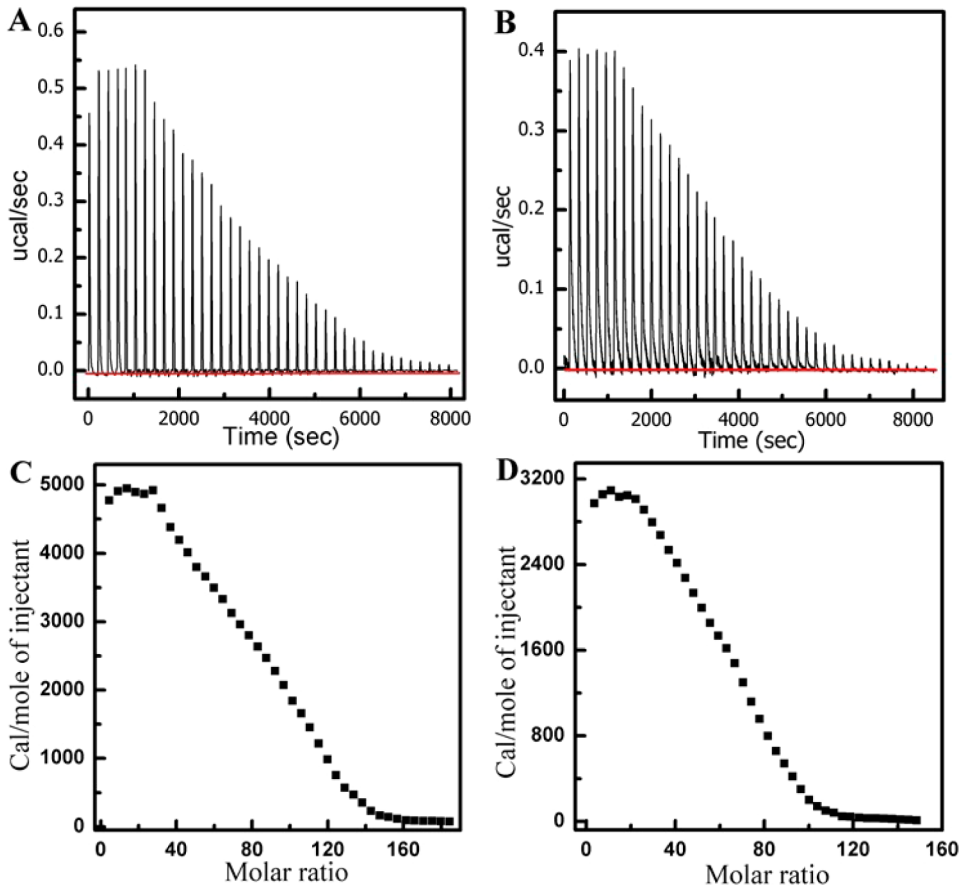

Figure 7. Isothermal calorimetry titration thermogram for (A) BSA-HA and (B) BLG-HA. Binding isotherm for (C) BSA-HA and (D) BLG-HA. Solvent (for both protein and polymer): 10 mM phosphate and 90 mM NaCl. Incremental volume of titrant: 6 μL; injection in 14.4 s.

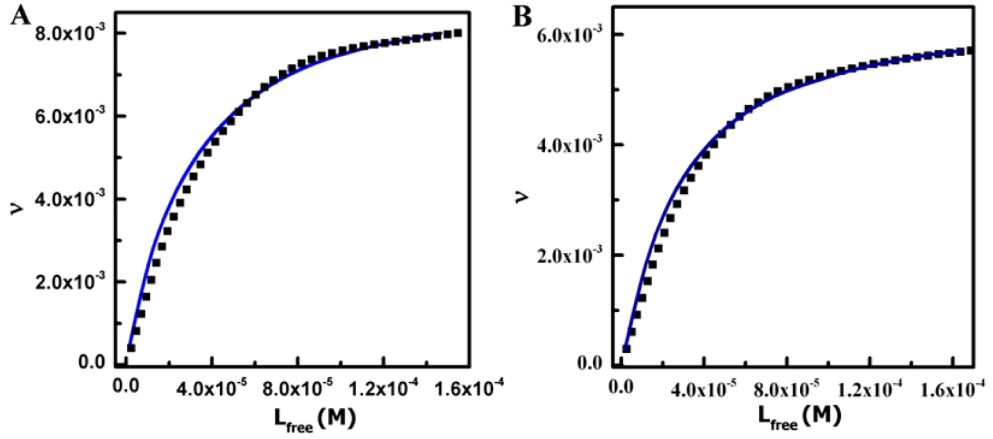

Figure 8. McGhee–Von Hippel fitting of (A) BSA-HA and (B) BLG-HA. Dotted lines are experimental binding isotherms; solid lines are nonlinear least-squares fitting by eq 1.

above 70%. The selectivity of the coacervation[38] can be described in terms of a selectivity ratio:

$$S = (P_A/P_B)'/(P_A/P_B) \quad (4)$$

where P is the SEC peak area, A and B designate the proteins (here BSA and BLG, respectively), and the prime designates the coacervate (vs supernatant). The value of S here for BSA/BLG is ~72, similar to the value found for coacervation with PDADMAC (~70), although the target protein in that case is BLG. For both forms of coacervation, that is, polyanion or polycation, separation occurs with simultaneous precipitation of BLG. Thus, the dense phase after centrifugation displays three layers: the upper two are optically clear fluids, identified as supernatant and coacervate, whereas the bottom layer is the solid precipitation of BLG (identified by the red color of RITC). Unlike coacervation, BLG precipitation is a kinetic as opposed to an equilibrium process; like coacervation, it depends on both pH and I. In the present case, the target protein BSA is concentrated in the coacervate. The "optimal pH, I condition" selected from the phase boundaries of Figure 3A, might adventitiously provide better separation by making

dx.doi.org/10.1021/bm500041a | *Biomacromolecules* 2014, 15, 726–734

Table 1. Thermodynamic Properties Obtained from Independent Site-Binding Model for Polymer−Protein Interactions[a]

polymer/protein	K_{obs} (M^{-1})	n	CL (nm)	ΔG (kcal/mol)	ΔH (kcal/mol)	$T\Delta S$ (kcal/mol)
HA/BSA[b]	389 ± 31	38 ± 1	49 ± 1	−3.53 ± 0.02	4.77 ± 0.01	8.30 ± 0.01
PDADMAC/BSA[c]	740 ± 30	80 ± 2	24 ± 1	−3.89 ± 0.02	−4.15 ± 0.02	−0.26 ± 0.03
HA/BLG[d]	228 ± 22	51 ± 1	66 ± 1	−3.21 ± 0.03	2.97 ± 0.01	6.18 ± 0.02
PDADMAC/BLG[e]	1900 ± 340	50 ± 1	15 ± 1	−4.5 ± 0.1	−4.67 ± 0.02	−0.2 ± 0.1

[a]Conditions for PDADMAC/Protein, HA/Protein is pH 5.3, I = 100 mM and pH 4.3, I = 100 mM, respectively, n is the binding site size (number of polymer units per bound protein molecule). [b]pH_c − pH = 0.7. [c]pH − pH_c = 0.7. [d]pH_c − pH = 0.5. [e]pH − pH_c = 0.9.

BLG unavailable for coacervation through its precipitation, but that process may be less easy to control.

Figure 3A indicates that selective coacervation cannot be obtained when pH_c values of the two proteins are identical. pH_c is qualitatively correlated in some way with binding affinity, in that, at any given pH, the protein with the higher value of pH_c will bind a polyanion more strongly. ITC measurements were conducted to quantitatively compare the thermodynamics of HA binding of BSA versus BLG. In the raw data of Figure 7, the vertical peaks correspond to the heat change in the cell containing HA at each protein injection. While the measurement of the heat of binding by ITC is straightforward, the values of entropy or energy obtained are model-dependent. The binding isotherm was fit by the overlapping binding site (McGhee von Hippel) model[27] previously applied to a number of protein−polyelectrolyte systems, notably BLG and pectin.[26] All thermograms directly measured from ITC were transformed to obtain the binding density ν and free protein concentration "L" values. The least-squares nonlinear curve fitting of ν plotted against L is also shown in Figure 8. Thermodynamic parameters n and K_{obs} values from the equivalent, independent, site-binding model are shown in Table 1. It is interesting to compare the protein affinity of HA with that PDADMAC, measured elsewhere.[2] On the basis of K_{obs}, PDADMAC binds more strongly to both BSA and BLG, by a factor ∼2 in the former and a factor of ∼9 in the latter. The primary cause may be the greater flexibility of PDADMAC, bare persistence length L_p^o = 2.5 nm[39] versus 4.2 nm for HA.[40] We also consider that PDADMAC with a distance between charges b = 7 Å has a linear charged density twice that of HA (b = 14 Å).

To continue this discussion of the higher affinity of PDADMAC, that is, $\Delta K = K_{obs}^{PDADMAC}/K_{obs}^{HA}$, we consider that ΔK is larger for BLG than BSA (i.e., 9× vs 2×). Why should the effect of chain flexibility or charge density of PE be more important for BLG? One possible answer is that the smaller protein BLG lacks a positive domain of low curvature,[15] which makes PE flexibility more important. The origin of the ΔK values, expressing stronger binding by PDADMAC regardless of protein, can be seen in Table 1 to arise from its more favorable binding enthalpy, which outweighs the more favorable $T\Delta S$ seen for HA. The correlation between a large favorable binding enthalpy and high affinity seems to be generally observed, so that complexes whose formation is driven only by entropy are usually ones of low affinity.[41] In our case, the higher flexibility of PDADMAC allows for a greater degree of exenthalpic ion-pairing. The lower value of $T\Delta S$ with PDADMAC can be attributed to the loss of PE configurational entropy upon PE/protein complex formation. As for HA/protein interactions, an unfavorable enthalpy might arise from inefficient ion-pairing due to the large spacing between polyanion charges particularly to pH < pK_{HA}. On the other hand, the loss of PE configurational entropy when the polyanion is constrained in the complex, might be less severe for this less flexible polymer, leading, together with counterion release, to a more favorable overall binding entropy. Finally, we can note that the difference in binding site sizes (number of polymer units per bound protein molecule), n = 50 and 37, can be expressed as binding site contour lengths (CL), 65 and 48 nm, for BLG and BSA, respectively, much larger than the respective protein diameters of 5.5 and 8.0 nm. Such large binding site sizes could arise from repulsive electrostatic interactions between neighboring proteins (anticooperative binding). On the other hand, it is noteworthy that CL varies inversely with K_{obs} and is always larger for HA. If the binding site were required to contain enough charges to neutralize the protein, HA with at most 1 charge per 13 Å would exhibit a large CL. We might then express n in terms of charges, with nz being the effective charge of a binding site where z is the charge per polymer unit. Low values of CL would be expected for PDADMAC because of the large number of polycation charges per unit contour length. Such small values for CL for HA would be insufficient to neutralize protein charge leading to the appearance of anticooperativity. The highest value of K_{obs} is observed for the polycation PDADMAC with the largest effective linear charge density[42] binding to BLG with the oppositely charged patch. The lowest value of K_{obs} is for HA with the lowest effective charge density binding to the protein (BLG) with the same-sign charge patch.

CONCLUSIONS

Selective binding of hyaluronic acid (HA) to BSA and BLG observed by differences in critical pH values for incipient binding and phase separation could be attributed in part to the opposite charge anisotropy of the two proteins. The values of pH corresponding respectively to the onset of complex formation, coacervation, precipitation, and redissolution, were determined as a function of ionic strength. The resultant phase boundaries for the two proteins were considered in terms of local and global protein charge, with a critical role also played by the charge on HA which diminished with decreasing pH while protein charge increased. It was proposed that complex formation, coacervation and precipitation were mainly influenced by protein charge anisotropy, net charge, and charged density, respectively. Optimal conditions for selective coacervation of BSA deduced from the phase boundaries, were found to yield this target protein with 90% purity from a 1:1 w/w mixture with BLG. Isothermal titration calorimetry verified the HA-affinity of BSA, twice that for BLG, as the origin of this separation. The preferential binding to PDADMAC, a flexible, high charge density polycation, was attributed primarily to a marked increase in favorable binding enthalpy for both proteins.

■ ASSOCIATED CONTENT

Supporting Information

Turbidimetric titration of HA with BSA, HA with BLG, and HA with BSA/BLG mixture in 100 mM NaCl. Turbidimetric titration of HA and BSA with and without BLG in 200 mM NaCl. Fluorescence image of FITC-BSA/RITC-HA coacervate suspension by confocal laser microscopy. This material is available free of charge via the Internet at http://pubs.acs.org.

■ AUTHOR INFORMATION

Notes

The authors declare no competing financial interest.

■ ACKNOWLEDGMENTS

The project was supported by the National Science Foundation (CBET-1133289, CBET-0966923) and MRSEC in UMASS. We thank Daniel Seeman and Dr. Julian McClements for assistance with protein modeling and isothermal titration calorimetry, respectively.

■ REFERENCES

(1) Kayitmazer, A. B.; Seeman, D.; Minsky, B. B.; Dubin, P. L.; Xu, Y. *Soft Matter* **2013**, *9*, 2553.
(2) Xu, Y.; Mazzawi, M.; Chen, K.; Sun, L.; Dubin, P. L. *Biomacromolecules* **2011**, *12*, 1512.
(3) Turgeon, S. L.; Schmitt, C.; Sanchez, C. *Curr. Opin. Colloid Interface Sci.* **2007**, *12*, 166.
(4) Sperber, B. L. H. M.; Schols, H. A.; Stuart, M. A. C.; Norde, W.; Voragen, A. G. J. *Food Hydrocolloids* **2009**, *23*, 765.
(5) Weinbreck, F.; de Vries, R.; Schrooyen, P.; de Kruif, C. G. *Biomacromolecules* **2003**, *4*, 293.
(6) Kamarck, M. E. *Nat. Biotechnol.* **2006**, *24*, 503.
(7) Nfor, B. K.; Ahamed, T.; van Dedem, G. W. K.; van der Wielen, L. A. M.; van de Sandt, E. J. A. X.; Eppink, M. H. M.; Ottens, M. *J. Chem. Technol. Biotechnol.* **2008**, *83*, 124.
(8) Meyer, V. R. *Practical High-Performance Liquid Chromatography*; Wiley: Chichester, U.K., 2010.
(9) Ghosh, R. *J. Chromatogr. A* **2002**, *952*, 13.
(10) Xia, J.; Mattison, K.; Romano, V.; Dubin, P. L.; Muhoberac, B. B. *Biopolymers* **1997**, *41*, 359.
(11) Mattison, K. W.; Dubin, P. L.; Brittain, I. J. *J. Phys. Chem. B* **1998**, *102*, 3830.
(12) Cooper, C.; Kayitmazer, A. B.; Turksen, S.; Dubin, P. L. *Curr. Opin. Colloid Interface Sci.* **2005**, *10*, 52.
(13) Antonov, M.; Mazzawi, M.; Dubin, P. L. *Biomacromolecules* **2009**, *11*, 51.
(14) Henzler, K.; Haupt, B.; Lauterbach, K.; Wittemann, A.; Borisov, O.; Ballauff, M. *J. Am. Chem. Soc.* **2010**, *132*, 3159.
(15) Grymonpre, K. R.; Staggemeir, B. A.; Dubin, P. L.; Mattison, K. W. *Biomacromolecules* **2001**, *2*, 422.
(16) Hattori, T.; Hallberg, R.; Dubin, P. L. *Langmuir* **2000**, *16*, 9738.
(17) Gök, E.; Olgaz, S. *J. Fluoresc.* **2004**, *14*, 203.
(18) Desfougeres, Y.; Croguennec, T.; Lechevalier, V.; Bouhallab, S.; Nau, F. *J. Phys. Chem. B* **2010**, *114*, 4138−4144.
(19) Goding, J. W. *J. Immunol. Methods* **1976**, *13*, 215.
(20) Harlow, E., Lane, D., Eds. In *Antibodies: A Laboratory Manual*; Cold Spring Harbor, NY, 1988; pp 353−355.
(21) Nicholls, A.; Honig, B. *J. Comput. Chem.* **1991**, *12*, 435.
(22) Tanford, C.; Kirkwood, J. G. *J. Am. Chem. Soc.* **1957**, *79*, 5333.
(23) Tanford, C.; Swanson, S. A.; Shore, W. S. *J. Am. Chem. Soc.* **1955**, *77*, 6414.
(24) Nozaki, Y.; Bunville, L. G.; Tanford, C. *J. Am. Chem. Soc.* **1959**, *81*, 5523.
(25) Tomme, P.; Creagh, A. L.; Kilburn, D. G.; Haynes, C. A. *Biochemistry* **1996**, *35*, 13885.
(26) Girard, M.; Turgeon, S. L.; Gauthier, S. F. *J. Agric. Food Chem.* **2003**, *51*, 4450.
(27) McGhee, J. D.; von Hippel, P. H. *J. Mol. Biol.* **1974**, *86*, 469.
(28) Raj, T.; Flygare, W. H. *Biochemistry* **1974**, *13*, 3336.
(29) Bhattacharya, M.; Mukhopadhyay, S. *J. Phys. Chem. B* **2012**, *116*, 520.
(30) Kaibara, K.; Okazaki, T.; Bohidar, H. B.; Dubin, P. L. *Biomacromolecules* **2000**, *1*, 100.
(31) Casal, H. L.; Köhler, U.; Mantch, H. H. *Biochim. Biophys. Acta* **1988**, *957*, 11.
(32) Staggemeier B. A. Studies of protein-polyelectrolyte binding: A comparison of biological and synthetic polyelectrolytes *Dissertation*, Purdue University, IN, 1999.
(33) Hayashi, K.; Tsutsumi, K.; Nakajima, F.; Norisuye, T.; Teramoto, A. *Macromolecules* **1995**, *28*, 3824.
(34) Muthukumar, M. *J. Chem. Phys.* **1987**, *86*, 7230.
(35) Odijk, T. *Macromolecules* **1980**, *13*, 1542.
(36) Cooper, C. L.; Goulding, A.; Kayitmazer, A. B.; Ulrich, S.; Stoll, S.; Turksen, S.; Yusa, S.; Kumar, A.; Dubin, P. L. *Biomacromolecules* **2006**, *7*, 1025.
(37) Boeris, V.; Romanini, D.; Farruggia, B.; Picó, G. *Process Biochem.* **2009**, *44*, 588.
(38) Wang, Y.; Gao, J.; Dubin, P. L. *Biotechnol. Prog.* **1996**, *12*, 356.
(39) Dautzenberg, H.; Goernitz, E.; Jaeger, W. *Macromol. Chem. Phys.* **1998**, *199*, 1561.
(40) Ball, V.; Winterhalter, M.; Schwinte, P.; Lavalle, Ph.; Voegel, J.-C.; Schaaf, P. *J. Phys. Chem. B* **2002**, *106*, 2357.
(41) Sperber, B. L. H. M.; Cohen Stuart, M. A.; Schols, H. A.; Voragen, A. G. J.; Norde, W. *Biomacromolecules* **2010**, *11*, 3578.
(42) Kayitmazer, A. B.; Shaw, D.; Dubin, P. L. *Macromolecules* **2005**, *38*, 5198−5024.